AD-A120 022 PENNSYLVANIA STATE UNIV UNIVERSITY PARK DEPT OF METE--ETC F/G 4/2
VALIDATION OF BULK TURBULENCE MODELING IN STABLE REGIMES.(U)
AUG 82 R E GOLUS, H A PANOFSKY N00014-81-K-0302
UNCLASSIFIED NEPRF-CR-82-09 NL

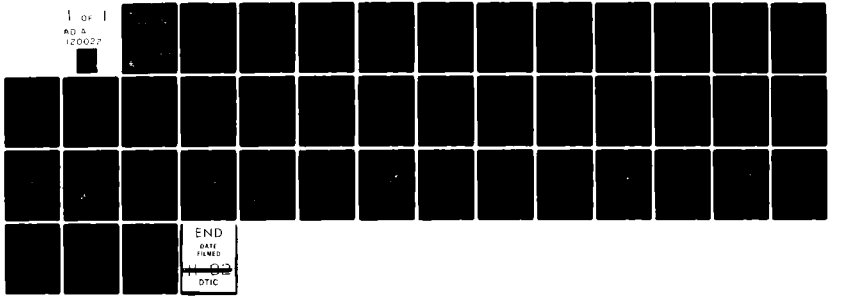

NAVENVPREDRSCHFAC
CONTRACTOR REPORT
CR 82-09

VALIDATION OF BULK TURBULENCE MODELING IN STABLE REGIMES

Prepared By:

Robert E. Golus and Hans A. Panofsky
The Pennsylvania State University
University Park, PA 16802

Contract No. N00014-81-K-0302

AUGUST 1982

APPROVED FOR PUBLIC RELEASE
DISTRIBUTION UNLIMITED

Prepared For:
NAVAL ENVIRONMENTAL PREDICTION RESEARCH FACILITY
MONTEREY, CALIFORNIA 93940

UNCLASSIFIED

SECURITY CLASSIFICATION OF THIS PAGE (When Data Entered)

REPORT DOCUMENTATION PAGE	READ INSTRUCTIONS BEFORE COMPLETING FORM
1. REPORT NUMBER: NAVENVPREDRSCHFAC Contractor Report CR 82-09 / 2. GOVT ACCESSION NO.: AD-A120042	3. RECIPIENT'S CATALOG NUMBER
4. TITLE (and Subtitle): Validation of Bulk Turbulence Modeling in Stable Regimes	5. TYPE OF REPORT & PERIOD COVERED: Final
	6. PERFORMING ORG. REPORT NUMBER
7. AUTHOR(s): Robert E. Golus & Hans E. Panofsky	8. CONTRACT OR GRANT NUMBER(s): N00014-81-K-0302
9. PERFORMING ORGANIZATION NAME AND ADDRESS: Department of Meteorology, The Pennsylvania State University, University Park, PA 16802	10. PROGRAM ELEMENT, PROJECT, TASK AREA & WORK UNIT NUMBERS: PE 62759N PN WF59-551, NEPRF WU 6.2-21
11. CONTROLLING OFFICE NAME AND ADDRESS: Naval Sea Systems Command, Department of the Navy, Washington, DC 20362	12. REPORT DATE: August 1982
	13. NUMBER OF PAGES: 42
14. MONITORING AGENCY NAME & ADDRESS(if different from Controlling Office): Naval Environmental Prediction Research Facility, Monterey, CA 93940	15. SECURITY CLASS. (of this report): UNCLASSIFIED
	15a. DECLASSIFICATION/DOWNGRADING SCHEDULE

16. DISTRIBUTION STATEMENT (of this Report)

Approved for public release; distribution unlimited.

17. DISTRIBUTION STATEMENT (of the abstract entered in Block 20, if different from Report)

18. SUPPLEMENTARY NOTES

19. KEY WORDS (Continue on reverse side if necessary and identify by block number)

Surface stress
Stability
Turbulence

20. ABSTRACT (Continue on reverse side if necessary and identify by block number)

A special set of observations of wind, temperature and moisture over Lake Ontario has been used to test bulk methods for computing stress, heat flux, evaporation, and structure constants, over a wide range of stabilities.

Reasonably good results were obtained for the structure constant of temperature (C_T^2). Bulk methods overestimated directly-measured stresses by about a factor of 2, possibly because wind speeds and wave speeds did not differ much from each other. ((Continued on reverse.))

DD FORM 1 JAN 73 1473 EDITION OF 1 NOV 65 IS OBSOLETE
S/N 0102-014-6601 |

UNCLASSIFIED

SECURITY CLASSIFICATION OF THIS PAGE (When Data Entered)

Block 20, Abstract, continued.

The moisture content was estimated correctly in near-neutral air, but the effect of stability variation was overestimated.

There was a good correlation between observed heat flux measurements and heat flux estimated by the bulk method, but the bulk estimates exceeded the Reynolds fluxes by an average of about 7-8 watts m^{-2}.

There are no systematic differences between bulk evaporation and Reynolds evaporation; but random scatter was considerable.

CONTENTS

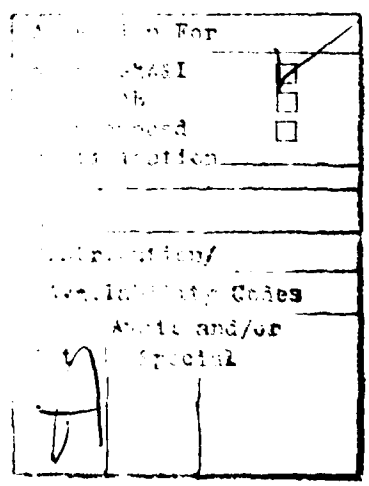

1. Introduction

In order to assess the characteristics of laser propagation above the sea, it is necessary to estimate the distribution of C_N^2, the structure constant for index of refractions.

The index of refraction depends primarily on temperature and moisture; in particular, we will see in Section 3 that

$$C_N^2 = c^2 C_T^2 \left[1 + \frac{0.06}{\beta} r + \left(\frac{0.03}{\beta}\right)^2\right]$$

where C_T^2 is the structure constant for temperature, β is the Bowen ratio and r is the correlation between high-frequency temperature and moisture fluctuations. c^2 is a known constant. If $r = 1$, this equation reduces to

$$C_N^2 = c^2 C_T^2 \left[1 + \frac{0.03}{\beta}\right]^2 .$$

On shipboard only relatively simple meteorological observations are usually available, e.g. wind, temperature and moisture at some height of order 10 m, and surface temperature.

Therefore, methods have been proposed to estimate C_N^2 and C_T^2 from such data, called "bulk methods". In particular, a method was suggested in NEPRF Tech. Rept: TR79-03, based largely on techniques suggested by Liu et al. (1979). Davidson et al. (1981) tested this method, but only over a small range of stability.

We discuss in this report an attempt to test the NEPRF bulk method (with slight modifications) on a more complete set of data, obtained by Donelan on a mast in Lake Ontario. He measured fluctuations of velocity

components, moisture and temperature as well as profiles of these variables during a wide range of stability conditions. Surface temperature was also available.

The purpose of the study was three-fold.

1. To test the NEPRF method for estimating C_T^2.
2. To evaluate the effect of moisture on C_N^2.
3. To test bulk methods for estimating the terms contributing to C_N^2 and C_T^2, that is, for estimating vertical flux of momentum, heat and moisture. These quantities, of course, have uses of their own, independent of their association with C_T^2 and C_N^2.

We will see that for various instrumental reasons, item (2) above was not resolved satisfactorily; but the other two items were.

2. Observations

2.1 General

During the 1972 International Field Year for the Great Lakes (IFYGL), experiments were conducted to measure vertical turbulent fluxes of momentum, heat, and moisture at the surface of Lake Ontario. Participants in these experiments included groups from the Canadian Center for Inland Waters (CCIW), the Atmospheric Environment Service, Canada (AES), the Bedford Institute of Oceanography, and many other groups from both Canada and the United States.

Mark Donelan, of the CCIW, obtained a data set which included fast-response measurements of the three orthogonal-wind components, temperature and humidity, as well as profile measurements of the mean wind, air temperature, humidity, and water temperature. These observations were made over a five-month period from mid-May to mid-September, thus covering a wide range of stabilities. It is this data set which is used to test a modified NEPRF

bulk model for the estimation of structure contrasts. In the same period, Canadian meteorological buoys, scattered over Lake Ontario (Figure 1a), recorded air and water temperature, wind speed, direction, and humidity at 10 minute intervals.

2.2 Site Description

Donelan's observations were taken at a location 2.6 km off the south shore of Lake Ontario and approximately 4 km west of the mouth of the Niagara River (Figure 1a). The sensor masts were supported by guy wires in 12 m of water. A barge, located approximately 170 m southwest of the masts (Figure 1b), housed the recording instruments which were connected to the sensors by cables. The center mast in Figure 1b was used for the turbulent fluctuation sensors while the mast 50 m to the east held the profile sensors.

This site offered long fetches with north to east winds. A list of the wind directions and their associated fetches is found in Table 1. Also, the nearness to shore made this site easily accessible by small boats.

A major concern about this location is its proximity to the mouth of the Niagara River. During late spring through early autumn, large horizontal surface temperature gradients are created where the water of the Niagara River empties into Lake Ontario. When the meandering of this "Niagara plume" brings it close to the measurement site, inhomogeneities arise in the surface layer due to the development of an internal atmospheric boundary layer. Since the bulk method is valid only under homogeneous conditions, cases in which inhomogeneities exist will give unreliable results. It is therefore, important to identify these cases.

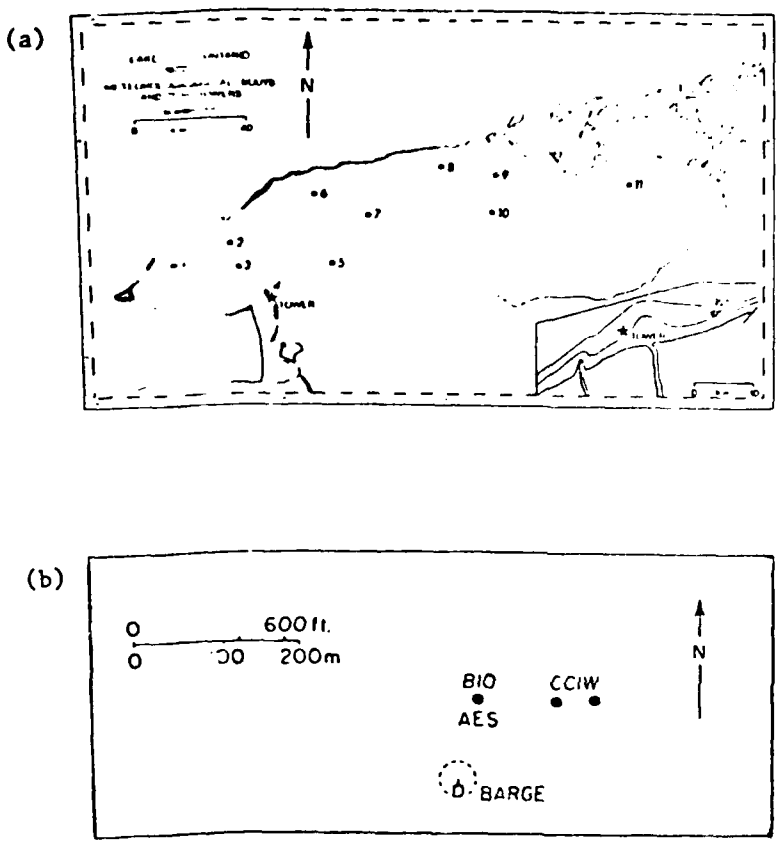

Fig. 1 (a) Outline of Lake Ontario showing the positions of the meteorological buoys and towers during IFYGL. (From Donelan et al. 1974). (b) Respective positions of towers and instrument barge. The two eastern towers were used by the CCIW. (From Smith, 1974).

No data were collected during periods of off-shore winds since the air is in a state of transition, and the fetch much too short for equilibrium conditions.

2.3 Instrumentation

Table 2 briefly describes the instrumentation employed for the turbulent fluctuation measurements. The variables were all sampled at a rate of 20 times per second.

Measurements of the three orthogonal wind components were made at a height of 9.55 m above the lake surface with an ultrasonic anemomenter-thermometer. The instrument was a model PAT-313A-1 with a model TR-31 probe, both manufactured by Marine Instrument Company, LTD., Tokyo, Japan. The measurement consisted of a pulse travel time differencing system across a probe span of 20 cm. See Mitsuta (1966) for a discussion of instrumental details. The instrument had a resolution of $\pm$ 2 cm sec^{-1} and frequency response of 1000 Hz.

Turbulent fluctuations of the temperature were measured in two ways: by the same anemometer-thermomenter described above; and a platinum wire sensor. The sonic anemometer-thermometer, at a height of 9.55 m, employed a pulse travel time summing method to measure the temperature fluctuations and had a resolution of $\pm$ 0.1°C and frequency response of 100 Hz. See Mitsuta (1966) for a discussion of the theory of the techniques.

The cold wire instrumentation consisted of a model 1040 temperature and switching module and a model 1210 standard straight platinum wire probe, both manufactured by TSI Incorporated, St. Paul, Minnesota. The wire sensor had a diameter of 0.004 mm, a length of 1.3 mm, and a frequency response of 5 k Hz. It was placed at 4.95 m and later moved to 9.55 m toward

Table 1. Wind directions and associated fetch.

direction	approximate fetch (km)
S	3
W	50
NW	40
N	60
NE	240

Table 2. Sensors used for turbulent fluctuation measureme

quantity	sensor
u	ultrasonic anemometer
w	ultrasonic anemometer
T	ultrasonic thermometer; platinum wire
q	lyman-alpha humidiometer
T_D	dewpoint hygrometer

Table 3. Sensors used for profile measurements

quantity	sensor
u	lightweight cup anemometer
wind direction	damped wind vane
T	thermistor
T_w	thermistor, submerged
q	standard radiosonde carbon hygristor

the end of the experiment. The instrument measured the electrical resistance of the wire, which is directly proportional to the temperature over small temperature ranges.

The turbulent humidity fluctuations were measured by a lyman-alpha humidiometer (LAH) in combination with a thermoelectric dewpoint hygrometer. The model BL lyman-alpha humidiometer used was manufactured by Electromagnetic. Research Corporation, College, Park, Maryland, and had a frequency response of 1500 Hz.

The LAH has a sensor tube which emits a beam of lyman-alpha radiation (λ = 0.00122 cm) through a lithium fluoride window, across a measuring path, through a second window, and into a detector. Due to the lyman-alpha absorption band of hydrogen, ambient water vapor in the measuring path decreases the beam intensity. The unabsorbed portion of the beam, upon entering the detector, ionizes the nitric oxide in the detector and generates a current according to the relation

$$I = c\, e^{-ax}$$

where I is the generated current, c is the constant, x is the path length, and a is the absorption coefficient for water vapor (380 cm^{-1}). The absorption coefficient for dry air is the order of 0.34 cm^{-1}. Therefore, I is essentially a measure of the water vapor density, q, in the measuring path. The output current decreases exponentially with an increase in q, but a logarithmic amplifier was used to produce a recorded signal varying linerly with q.

Lithium fluoride was used in the sensor as window material due to its high transmissivity of lyman-alpha radiation. A disadvantage of this

material is that it is soluble in water, so that sea spray or condensation on the windows will etch them and, therefore, lower their transmissivity. For this reason, a dewpoint hygrometer was used in conjunction with the LAH for constant calibration.

The calibration between the two instruments was done during the data analysis. Also, both instruments were at the same height for all the runs analyzed. Of course, the response of the hygrometer is too slow for measurements of humidity fluctuations at high frequencies.

The dewpoint hygrometer system used was a model 137-C1, Vapor Mate II with a model 137-C2 sensor, both manufactured by Cambridge Systems, Waltham, Massachusetts. This instrument employed a cooled mirror which was warmed by condensation of ambient water vapor. A precision thermistor measured the temperature change. The output of the thermistor, being a nonlinear function of temperature, was linearized through a bridge circuit.

The profiles were measured on a tower 50 m to the east of the location of the measurements of the turbulent fluctuations. The wind direction was also measured at a height of 15 m above the lake surface. The mean wind speed, temperature, and humidity were measured at fixed levels of 12.1 m, 8.0 m, 5.2 m, 3.4 m, and 2.1 m. The water temperature was measured a few centimeters below the water surface to yield a "bucket temperature". A brief description of the sensors used for the profile measurements is found in Table 3. Mean values of the measurements at the start and end of consecutive 10 minute intervals were determined. Donelan et al. (1974) gives a detailed description of the sensors.

During the first three months of this experiment, profile measurements of humidity were not available due to problems with the carbon hygristor. Instead, mean dewpoint temperatures from the dewpoint hygrometer on the center tower at 9.55 m were used.

There were also eight periods in which turbulent fluctuation measurements were available while profile measurements were not. During these periods, bulk methods were based on measurements at the nearby buoy #4.

2.4 Analysis

The turbulent fluctuations were recorded on two different FM tape recorders in analog form and later digitized at 20 Hz for analysis by computer. Time series were recorded on a plotter and later used to identify good segments of data to be used as individual runs. A run was usually terminated at a point just before any one of the sensors reached saturation which is when the recorded signal from a sensor goes off-scale. Time series which did not reach saturation were usually of long duration and were divided into two or more separate runs. Table 4 shows the number, and duration of each run, as well as special characteristics of each run.

Once the runs were defined, analysis of the data was performed on a Cyber 171 computer system at the CCIW. The Cyber 171 utilized a fast-fourier tranform scheme to produce spectra cospectra, and quadrature spectra of the three orthogonal-wind components, sonic temperature, and humidity. The platinum wire temperature fluctuations could not be correlated with any of the sonic or humidity fluctuations since they were recorded on a different tape recording system. Therefore, only one-dimensional temperature spectra were obtained from the wire data, and the instrument could not be used for estimating the heat flux.

The cospectra yielded direct measurements of the fluxes while the one-dimensional temperature and moisture spectra were used to determine the structure constants.

The one-dimensional horizontal-wind spectra were also used to determine the momentum flux (stress) through the dissipation method. The different estimates of the fluxes and structure constants will be compared with the bulk estimates in Chaper 4.

A discussion of the analysis techniques for the raw profile data appears in Donelan et al. (1974). Mean values of wind speed, air temperature, and humidity were available for the five fixed levels mentioned in Section 2.3.2 along with the water temperature. As was mentioned before, humidity profiles were available only during the later runs. Since the NEPRF bulk model requires the mean wind at 10 m for estimating roughness lengths, a reference height of 10 m was chosen. Since the variables were usually available at 8 and 12 m, estimates for 10 m could be made by simple interpolation.

For several stable runs profile information was not available. For these cases, a reference height of 3.6 m was chosen for the NEPRF bulk model since this corresponds to the height at which the buoy measurements were taken. However, the model still required the mean wind at 10 m for the estimation of roughness lengths. To obtain an approximate 10 m wind speed, the 4.0 m wind was multiplied by a factor of 1.2. This multiplication factor was obtained from the average ratio of 10 m to 4 m winds during stable periods with complete wind information. Although this factor is a function of stability, these estimated 10 m wind should give satisfactory estimates of the roughness lengths, which do not vary much over small ranges of wind speed.

Tables 4 and 4a list the runs used and their idiosyncrasies.

Run	1972 Date	Duration (min)	Data Code (see Table 4a)	Run	1972 Date	Duration (min)	Data Code (see Table 4a)
3	May 22	24	A	21-1	27	58	B
4	22	26	A	22	June 16	15	B
4-1	22	26	A	22-1	16	21	B
5	24	30	A	23	16	46	A
6	24	31	A	24	19	39	B
6-1	24	18	A	25	21	32	A
7	24	24	A	26	22	11	A
7-1	24	23	A	27	24	63	A
8	25	45	A	30	Aug. 25	90	D
9	25	13	A	31	31	82	C
10	25	53	A	32	Oct. 5	17	C
11	25	27	A	33	12	54	E
12	25	51	A	34	13	40	E
13	25	43	A	34-1	13	40	E
14	25	44	A	35	13	50	E
15	26	18	A	35-1	13	47	E
16	26	61	A	36	13	64	E
18	26	91	A	37	13	43	E
19	27	47	B	37-1	13	36	E
20	27	19	B	37-2	13	36	E
21	27	29	B	38	13	20	E

Table 4. Date and duration of each run used for analysis, and data codes defined in table 4a.

Table 4a

Data Code	Fast-Response Sensor Height 4.95 m	9.55 m	Profile Information Available
A	Cold Wire	Ultrasonic, LAH	Yes
B	Cold Wire	Ultrasonic, LAH	No
C		Ultrasonic, LAH, Cold Wire	Yes
D		Ultrasonic, LAH, Cold Wire	No
E		LAH Cold Wire	Yes

3. Theory

3.1 General Characteristics of C_N

Let N be the index of refractions for the wave length used in a laser. Then the structure function for this index is defined by (x is a position variable):

$$D_N(r) = \overline{[N(x) - N(x + r)]^2}$$

Here an overbar should represent an ensemble average. In practice it is taken as a space average.

If the turbulence is homogeneous, D_N depends on separation r only. For small r ($r << z$, the height), we can use Kologorov theory:

$$D_N(r) = a\varepsilon^{-1/3} \chi_N r^{2/3}$$

Here "a" is a constant, about 3; ε is the dissipation of turbulent energy, and χ_N is the rate of destruction of $\overline{N'^2}/2$ by molecular action (where N' denotes the deviation from an average).

The quantity $a\varepsilon^{-1/3} \chi_N$ is defined as the structure "constant", and denoted by C_N^2. Given C_N^2, the interaction between turbulence and laser beams can be evaluated by the "classical" theory derived by Tatarski (1971).

If Monin-Obukhov theory is adequate, dimensional analysis gives:

$$C_N^2 = N_*^2 z^{-2/3} g (z/L) \qquad (1)$$

where g is a universal function. N_* is defined (in analogy with T_*) by:

$$N_* = - \frac{\overline{w'N'}}{u_*} \qquad (2)$$

Here w is the vertical velocity, and $T_* = - \frac{\overline{w'T'}}{u_*}$. The minus sign in this definition is arbitrary, and added so that T_* has the same sign as Richardson number, and Monin-Obukhov L, defined by $L = \frac{-u_*^3 C_p \rho T}{kg\ H} \left(1 + \frac{.07}{\beta}\right)^{-1}$, where k is the vonKarman constant and β is the Bowen ratio; C_p the specific heat at constant pressure; g, gravity and H, the vertical heat flux.

Now, N' is given by aT' + bq' where a and b are known parameters which are constant for practical purposes. q is the specific humidity. Hence, equ. (2) becomes

$$- N_* = a \frac{\overline{w'T'}}{u_*} + b \frac{\overline{w'q'}}{u_*} = - aT_* - bQ_* \qquad (3)$$

where Q_* is defined as $- \overline{w'q'}/u_*$.

Hence,

$$N_* = + a\ T_* \left[1 + \gamma \frac{Q_*}{T_*}\right] \qquad (4)$$

where $\gamma = b/a$.

But $\frac{Q_*}{T_*} = C_p/\ell\beta$

where β is the Bowen ratio and ℓ the latent heat.

Hence,

$$N_* = + T_* \left[1 + \frac{\gamma C_p}{\ell\beta}\right] \qquad (5)$$

C_T^2 is defined through the structure function and Kolmogorov theory in analogy with the definition of C_N^2. Therefore, we can put (see Wyngaard, et al., 1971).

$$C_T^2 = T_*^{-2} z^{-2/3} f(z/L) \tag{6}$$

If f(z/L) is the same universal function as g(z/L) above, equations (1) and (5) combine to form

$$C_N^2 = a^2 (T^2 [1 + \frac{\gamma C_p}{\ell \beta}]^2) \tag{7}$$

The ratio $\frac{\gamma C_p}{\ell}$ is 0.03 for lasers.

Hence, finally

$$C_N^2 = a^2 C_T^2 [1 + \frac{0.03}{\beta}]^2 \tag{8}$$

If this equation were correct, only estimates of C_T^2 and Bowen ratio would be needed to obtain C_N^2. However, equ. 8 is controversial. McIlveen (1981) derived instead (see also Wesely, 1976)

$$C_N^2 = C_T^2 [1 + \frac{.06}{\beta} r + (\frac{.03}{\beta})^2] \tag{9}$$

Where r is the correlation coefficient between moisture differences and temperature differences at points with small separations. If r = 1, or -1, equations 8 and 9 coincide, since r will have the same sign as β.

We had hoped to test the correlations between temperature fluctuations and moisture fluctuations in this project. But only sonic temperatures

were measured at the same times and nearly the same place as moisture. And, as we will see, the sonic temperature spectra were extremely noisy and unreliable. We expect r^2 to be close to 1, so that the difference between equations 8 and 9 is not important.

In most cases, the influence of moisture on C_N^2 is expected to be small. In only 2 of the 41 cases for which bulk Bowen ratios were computed, the absolute value of β was less than 0.1. Also, in 2 cases, $|\beta|$ exceeded 1. Hence, usually, the difference between equations 8 and 9 is not of critical importance, over Lake Ontario. This does not mean that the effect of moisture is always unimportant over Lake Ontario: in the two cases in which β was less than 0.1, the moisture effect should not be neglected in the evaluation of C_N^2. But, in these cases, C_T^2 was quite small.

Here, we will concentrate here on C_T^2. We will begin with equ (6), written in the form

$$C_T^2 = \left(\frac{\overline{w'T'}}{u_*}\right)^2 g(z/L) z^{-2/3} \qquad (10)$$

As we have seen, the length L depends only on $\overline{w'T'}$, $u_* \equiv -\overline{u'w'}$, and β, which also depends on $\overline{w'q'}$ and $\overline{w'T'}$.

Hence, we will first consider bulk methods to determine $\overline{w'T'}$, $\overline{w'u'}$, and $\overline{w'q'}$, from ship-board data.

3.2 Bulk methods for stress

For aerodynamic flow, $\overline{u'w'}$ is usually described by:

$$-\overline{u'w'} = \frac{k^2 u_z^2}{\left(\ln\frac{z}{z_o} - \psi\left(\frac{z}{L}\right)\right)} \qquad (11)$$

where u_z is the wind speed at height z, z_o is the roughness length, and ψ is a presumably universal function which is quite well known and has been

tabulated. It is negative in stable air and positive in unstable air. The factor $k^2/(\ln z/z_o - \psi(\frac{z}{L}))^2$ is often called the "drag coefficient", Γ_m.

There is some disagreement as to the choice of z_o. It is usually between 0.01 and 0.5 cm and increases with increasing wind speed. Different investigators have derived somewhat different relationships between z_o and wind speed. In this work, we have made use of three different relations, suggested, respectively, by Liu et al. (1979), Smith and Banke (1975) and Garratt (1977). The differences between these three formulations are not very great. More serious is the problem that the stress, $-\rho\ \overline{u'w'}$, should not only depend on the wind speed, roughness and stability, but also on the difference between wind speed and wave speed--which depends on the "age" of the wave; in well-developed waves with large fetch, wave speed and wave speed can be very similar, reducing the stress below that expected from equation (11).

In order to evaluate the stress by equ (11), we employ a process of successive approximations, which converges rapidly in practice. We first estimate $\overline{u'w'}$ for neutral conditions, and use the corresponding technique to infer $\overline{w'T'}$ from air-sea temperature difference and temperature roughness length for $\psi = 0$ (see next section). Given $\overline{w'T'}$ and $\overline{u'w'}$, we compute L and hence $\psi(\frac{z}{L})$ and recompute $\overline{u'w'}$ and L. This procedure usually has to be repeated only twice to yield stable estimates of $\overline{u'w'}$.

3.3 Bulk method for heat flux

For heat flux, Monin-Obukhov theory suggests:

$$\overline{w'T'} = \frac{k^2(\theta_s - \theta_z)u_z}{[\ln \frac{z}{z_{o_T}} - \psi_h(\frac{z}{L})]\ [\ln \frac{z}{z_o} - \psi(\frac{z}{L})]} \qquad (12)$$

where θ_z is the (potential) temperature at height z and θ_s is the surface temperature. Again, the function $\psi_h(\frac{z}{L})$ is well known. One difficulty with the use of (12) is that θ_s is the "skin" temperature, whereas "bucket" temperatures are usually measured. The bucket temperature can be significantly warmer than the skin temperature

In order to correct for the possible effect of this difference, Liu et al. (1979) have constructed a nomogram which permits estimates of differences between skin and bucket temperatures from wind speed and differences between air and bucket temperatures. We use the results of this nomogram in the numerical form suggested by Burk et al. (1979).

Another problem is the interpretation of z_{oT}. This is not really a function of ocean roughness, but a measure of the molecular transfer of heat through the surface. It is of order ν/u_* where ν is the molecular heat conductivity. We use here the estimate of z_{oT} based on Liu et al.'s relations under neutral conditions as functions of wind speed.

We then proceed to solve equ 12 first for $\psi_h = 0$. This is combined, as before, with $-\overline{u'w'}$ computed for z/L = 0, to form L. Hence the computations of $\overline{w'T'}$ is repeated several times leading to presumably improved estimates of L.

3.4 Evaporation

Although $\overline{w'q'}$ is not usually important for C_N^2, bulk estimates of evaporation are important for other reasons. Further the effect of $\overline{w'q'}$ on C_N^2 cannot be neglected over tropical oceans. In analogy with equations (11) and (12), we then have:

$$\overline{w'q'} = \frac{k^2(q_s - q_z)u_z}{[\ln \frac{z}{z_{oq}} - \psi_q(\frac{z}{L})]\ [\ln \frac{z}{z_o} - \psi(\frac{z}{L})]} \qquad (13)$$

Here, q_s, the surface specific humidity, is evaluated from the surface skin temperature; ψ_q is equated with ψ_h and z_{oq} is also obtained from Liu et al. (1979). Then, equ. 13 is solved by successive approximations, initially with $L = \infty$, and then with progressively more realistic L-values.

This whole procedure is analogous to that suggested by Burk et al. (1979) except that z_o, z_{oT} and z_{oq} are assumed to depend on wind, and not on stability. Thus, these parameters are not changed in successive iterations.

3.5 Other techniques for estimating fluxes and structure constants

The quantities $-\overline{u'w'}$ could be estimated directly from observations of fluctuations of u and w. However, the results are extremely sensitive to errors in tilt of the mast.

Another technique, depending on accurate high-frequencies recording (frequency > 1 hz) is based on Kolmogorov theory:

$$k_1 S(k_1) = c\, \varepsilon^{2/3} \left(\frac{f}{u}\right)^{-2/3} \tag{14}$$

where S is the spectral density at longitudinal wave number k_1, c is a universal constant, f, frequency, and ε, as before, energy dissipation into heat.

For Monin-Obukhov scaling, ε is described by:

$$\varepsilon = \frac{u_*^3}{kz}\ \psi_\varepsilon \tag{15}$$

We use here $\phi_\varepsilon = 1 - \frac{z}{L}$ in unstable air, and $\phi_\varepsilon = [1 + 2.5\ (\frac{z}{L})^{.6}]^{3/2}$ in stable air. Hence, if we eliminate ε between equ. (15) and (14) we derive an equation for $u_*^2 = -\overline{u'w'}$.

$\overline{w'q'}$ and $\overline{w'T'}$ were measured from their definitions only, although there exist methods to infer them from high-frequency fluctuations of q and T, respectively, once ε or u_* are given.

C_T^2 was estimated from high-frequency temperature spectra (k_1 in radians per unit length):

$$S_T(k_1) = 1/4\ C_T^2\ k_1^{-5/3}$$

with Taylor's hypothesis that $k_1 = \frac{2\pi f}{u}$ (f in hz).

An attempt was also made to estimate C_N^2 for sound from the analogous equations for index of refraction for sound:

$$S_N(k_1) = \frac{1}{4}\ C_N^2\ k_1^{-5/3} \quad ,$$

making use of the spectra of the sonic thermometers, in order to check equ. (9).

4. Results

4.1 Heat flux

Figure 2 compares directly measured $\overline{w'T'}$ with $\overline{w'T'}$ estimated from the ulk method (equ. 12). Since only sonic temperatures could be used, the unstable cases of October are not included. The sonic temperatures had been corrected for moisture and wind effects. The general agreement is surprisingly good. There are a few cases with generally small heat flux, when the directly measured Reynolds flux was negative, but the bulk heat flux was positive. For some of these cases, temperature profiles were available. These showed that the air was slightly stable around 10 m where $\overline{w'T'}$ was measured, in agreement with the negative sign of $\overline{w'T'}$. But the surface temperature was larger than the temperature at 10 m leading to upward heat flux by the bulk method. This kind of profile is not homogeneous but suggests that the lowest layers had been warmed, perhaps when the air drifted over the near-by warm Niagara plume.

If the bulk method value of flux had been computed from a surface temperature, extrapolated downward from the profile, the bulk fluxes would also have been negative and in good agreement with measured $\overline{w'T'}$. For large downward flux, there appears a tendency for the bulk flux to be larger in absolute value than $\overline{w'T'}$. On the average there is a slight bias in the sense that bulk heat fluxes exceed Reynolds heat fluxes by about 7 watts m^{-2}. The reason for this bias is not known. Both the corrections for wind and moisture fluxtuations are in the wrong direction, so that the agreement could have been improved slightly if these corrections had not been made.

4.2 Stress

Figure 3 shows estimates of $\tau/\rho = -\overline{u'w'}$. Bulk results are shown along the abscissa, direct Reynolds stress measurements and ε results along the

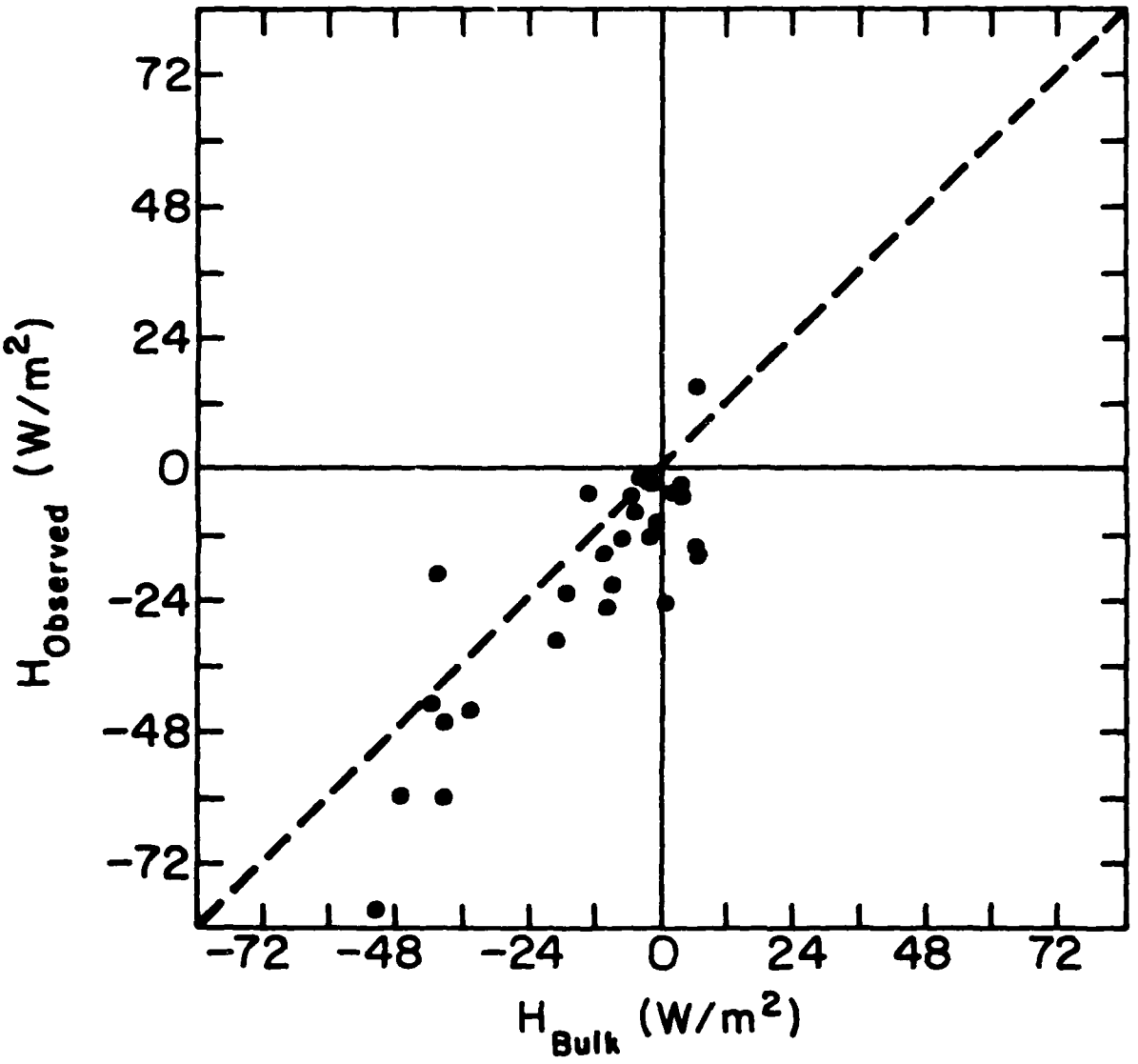

Fig. 2 Comparison of sensible heat fluxes from eddy-correlation method and bulk method.

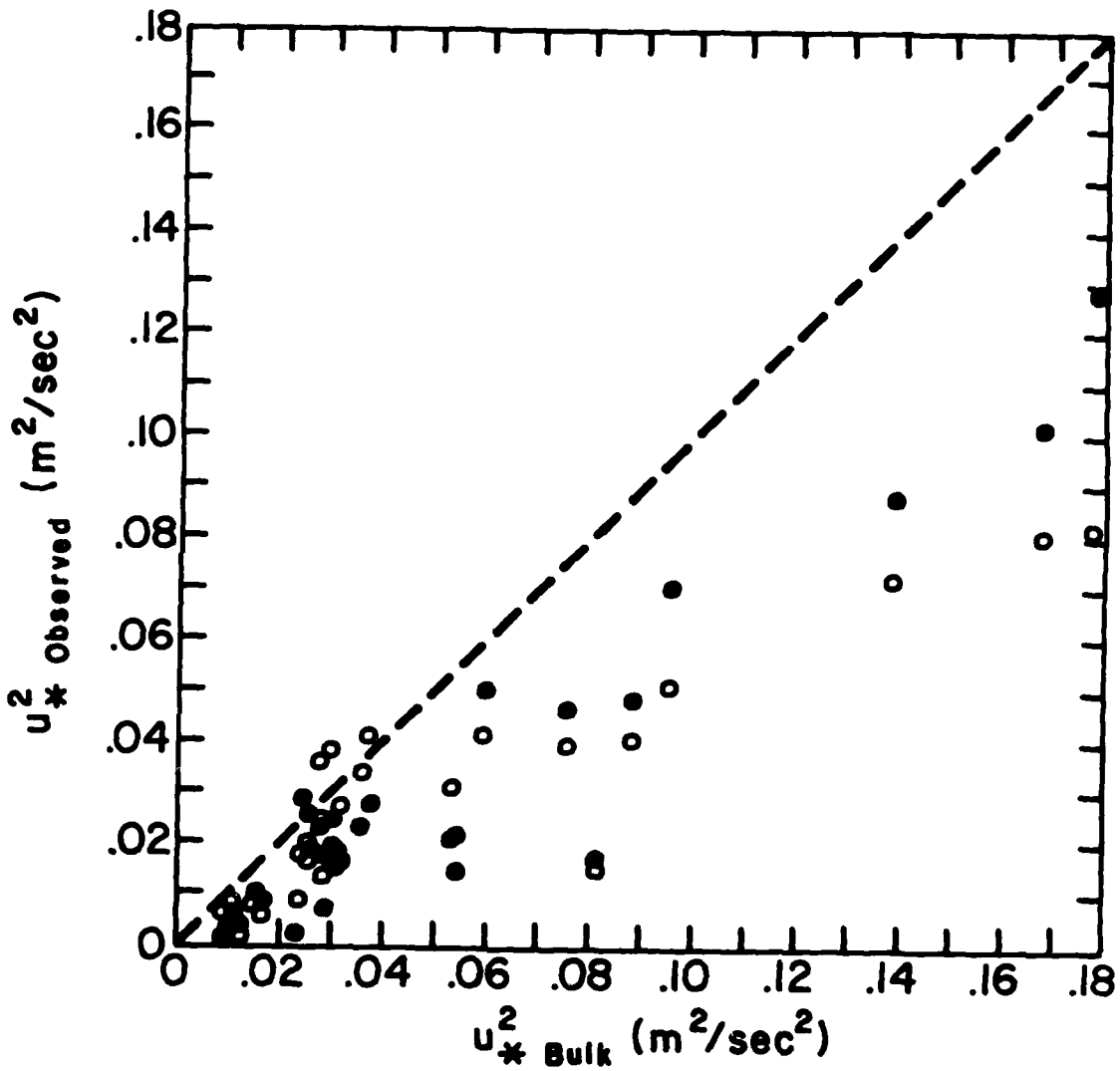

Fig. 3 Comparison of momentum fluxes from eddy correlation method (dots) and dissipation method (circles) with bulk method.

ordinate. Again, Reynolds stresses and dissipation stresses had to be based on sonic anemometers, so that the unstable cases in October are not included in this figure. For a fixed bulk estimate, the observed stresses by dissipation and direct methods are not usually far apart. We therefore suggest that the best estimates of "true" stresses are close to these measurements.

For $u_*^2 < 0.04\ m^2\ sec^{-2}$, the agreement between bulk methods and the others is reasonably good. Even then, the bulk estimates (derived from the work of Liu, et al. (1979) tend to be relatively large. But in cases of large stresses (strong winds) the bulk methods seem to overestimate stresses by about a factor of 2 (or u_* by $\sqrt{2}$).

The reason is not clear. Possibly, in a well-developed wave pattern with large fetch, wave speeds in strong winds are not very different from wind speed, thus producing a small stress for a given wind.

To test this hypothesis, we plotted the differences between bulk stress and Reynolds stress as function of wind direction and speed; the fetch was a strong function of wind direction, with longest fetches with North winds and shortest for South winds (see Table 1).

Figure 4 shows the results. Indeed, largest differences between bulk and Reynolds stresses occur with strong winds at 10 m with large fetch, suggesting that small drag coefficients are appropriate in these cases because of the small differences between wind speed and wave speed. Note that these strong winds were directly measured, not extrapolated vertically from 4 m.

Since, apparently, bulk estimates overestimate u_*, they should also seriously overestimate L, which is proportional to u_*^3.

4.3 Moisture flux

Figure 5 compares bulk and Reynolds moisture flux. The result is quite satisfactory with no strong bias suggested. There is a slight tendency, for the bulk methods to overestimate the fluxes when $\overline{w'q'} < 1 \frac{cm}{sec} \frac{gm}{kg}$. For

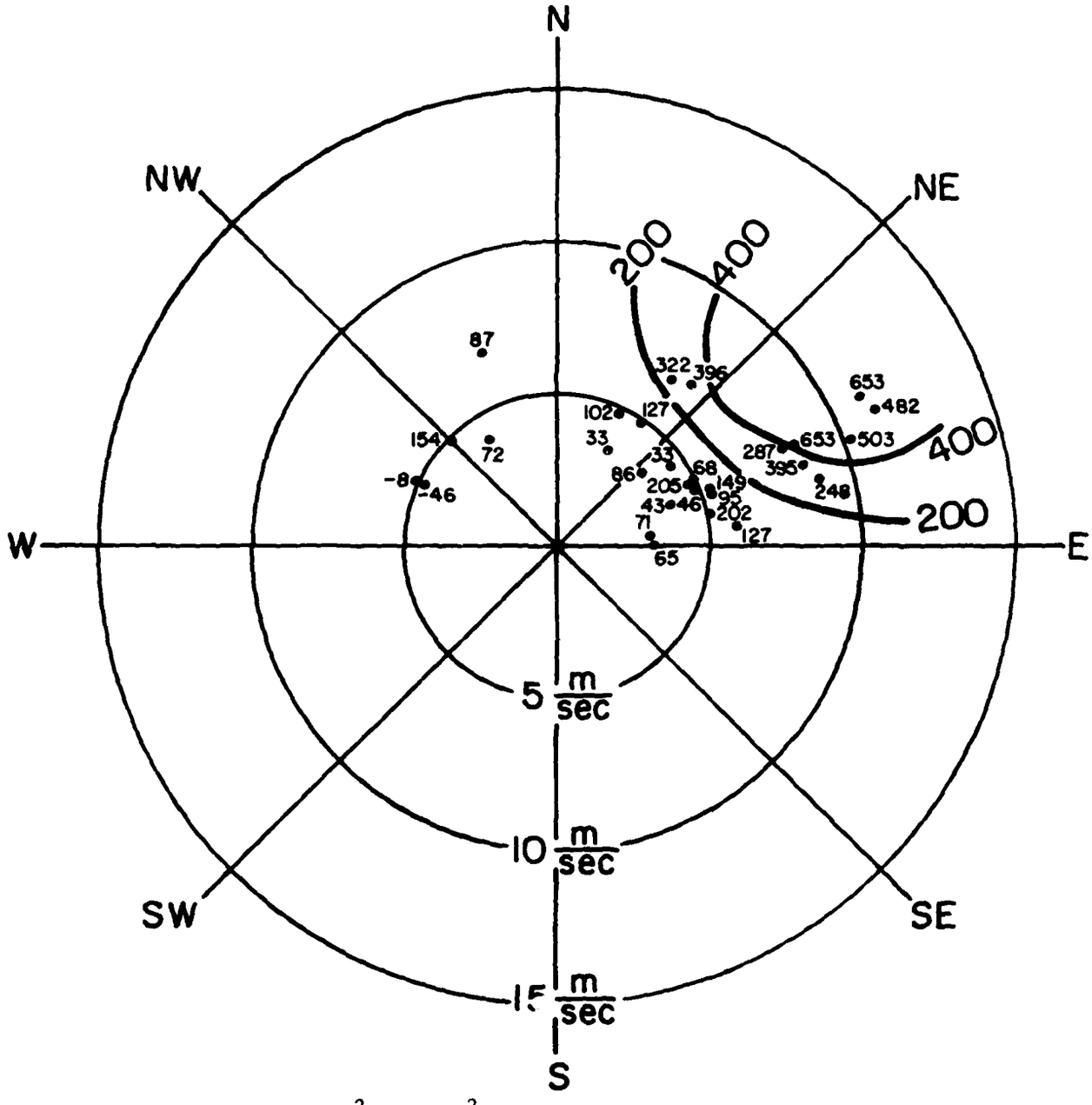

Fig. 4 $(u_*^2{}_{bulk} - u_*^2{}_{observed})$ vs. wind speed and direction at 10 m. u_*^2 is in $cm^2\ sec^{-2}$.

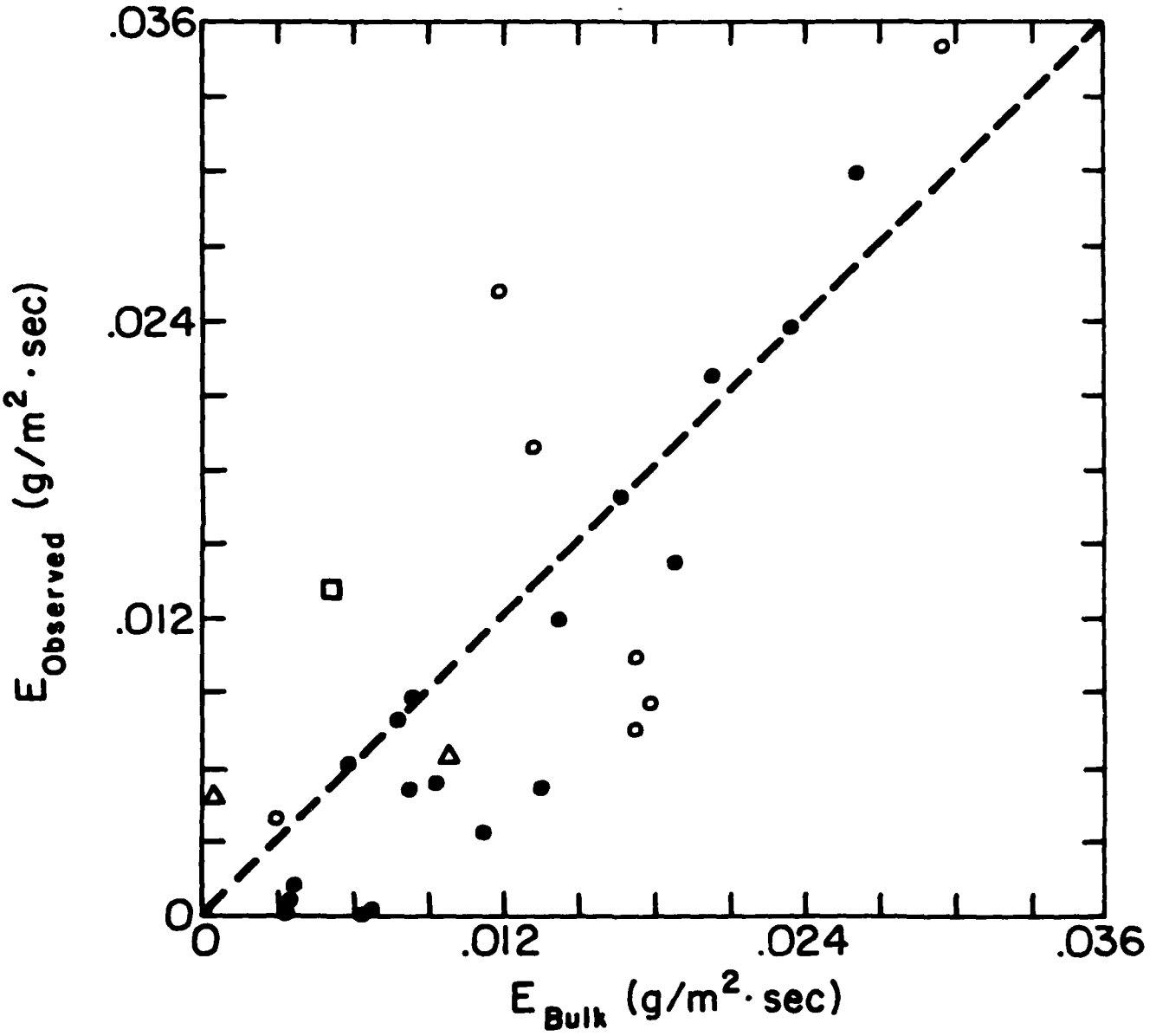

Fig. 5 Comparison of moisture fluxes from eddy-correlation method and bulk method. Stable periods are represented by dots; unstable by squares; neutral by triangles; and cases when the observed and bulk sensible heat fluxes have opposite signs by open circles.

larger fluxes, no bias is obvious. However, there is considerable random scatter, Note, that, again the unstable cases of October are excluded.

4.4 C_T^2 and C_N^2

Figure 6 compares bulk estimates of C_T^2 with C_T^2 estimated from temperature spectra. The agreement is especially good when $C_T^2 > 2 \times 10^{-3} \circ C^2 z^{-2/3}$, both for stable and unstable air. For very small C_T^2, the spectral estimates are significantly higher than the bulk estimates. We believe this is due to noise in the spectral data; since spectra are positive definite, any "noise" will produce net positive errors. Also, some of the worst discrepancies occur for cases where the bulk heat flux and measured heat flux had opposite sign, so that the basic conditions for bulk methods were not satisfied.

The good agreement between "observed" C_T^2 and bulk C_T^2 may appear surprising in view of the poor performance of bulk methods for estimating stress. The reasons may be these:

First, the determination of the quantity $T_* = -\frac{\overline{w'T'}}{u_*}$ by bulk methods is independent of the drag coefficient of momentum. This is because the temperature profile is given by:

$$\frac{T - T_o}{T_*} = \ln \frac{z}{z_{oT}} - \psi_h \left(\frac{z}{L}\right)$$

The bulk method determines T_* from this equation. The drag coefficients comes in only weakly through $\psi_h \left(\frac{z}{L}\right)$, since L depends on stress. But because the incorrect drag coefficients occur with strong winds, ψ_h is small compared to $\ln z/z_{oT}$ in these cases.

The drag coefficient enters the estimation of C_T^2 also through the function g(z/L) in equ. 10. But again, the doubtful drag coefficients occur for strong winds, where $g(z/L) \sim g(0)$ which does not depend on stress.

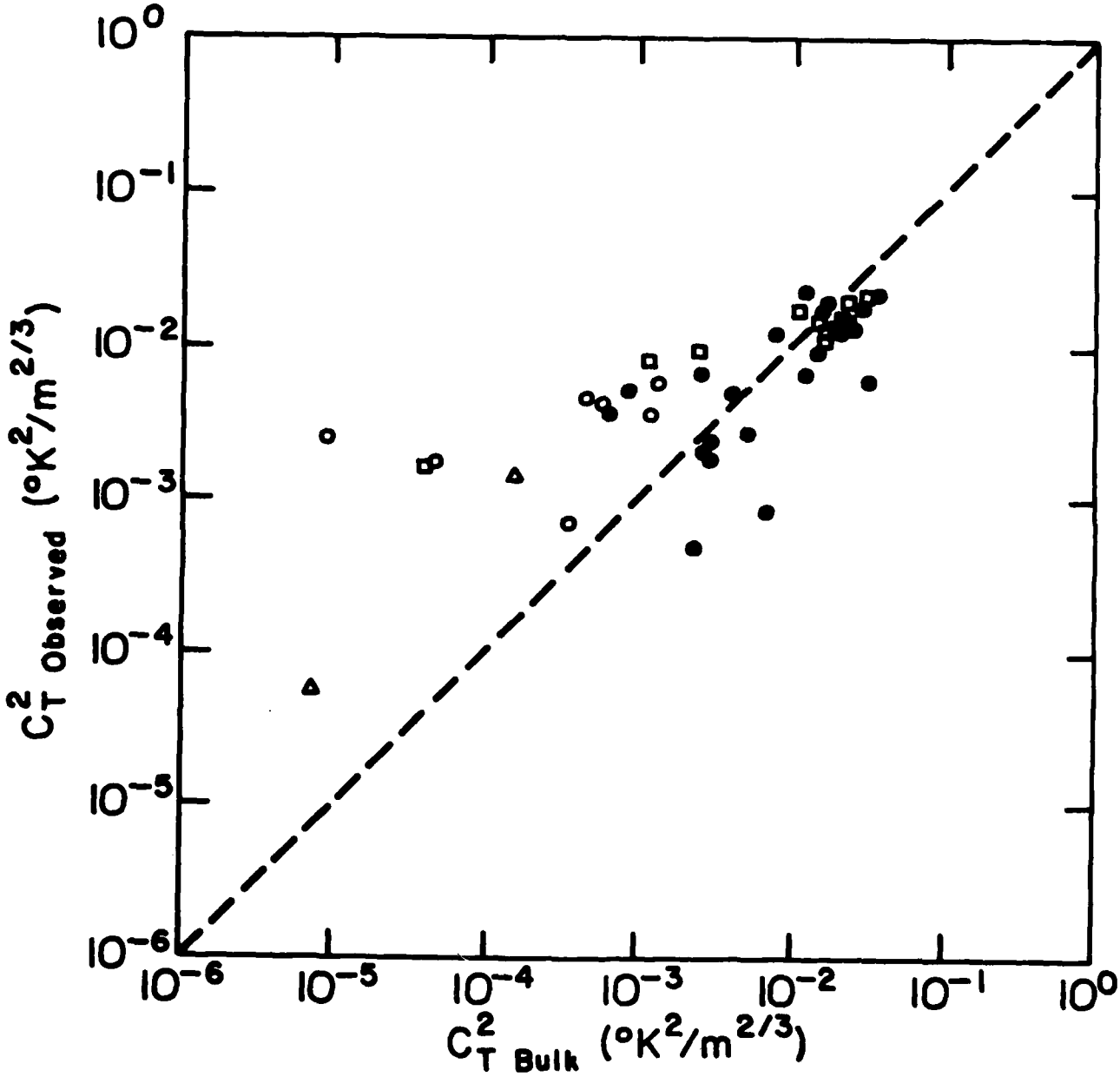

Fig. 6 Comparison of temperature structure constants from one-dimensional temperature spectra and the bulk model. Dots, stable; squares, unstable; triangles, neutral; circles, bulk and Reynolds fluxes have opposite sign.

There probably is little advantage in applying moisture corrections as suggested by equations (8) or (9) in order to calculate C_N^2, for observations such as those available here. The reason is that the corrections depends on the Bowen ratio. But here, any Bowen ratio estimated by bulk methods may not even agree in sign with the actual Bowen ratio, when conditions are not homogeneous. E.g. sometimes, when $T_s > T$, the bulk heat flux is upward, yet the local heat flux at 10 m is down. Moisture flux is upward, in all cases, so that the bulk Bowen ratio has the wrong sign.

4.5 Comparison of sonic and wire temperature spectra

Sonic thermometers actually measure spectra of the index of refraction for sound. This is proportional to the speed of sound given by $20.1\sqrt{T(1 + .51q)}$. A fluctuation of T_s, T_s', is then approximately given by

$$T_s' = T' + .51\,\overline{T}\,q' \quad .$$

If the correlation between q' and T' is high, in absolute value, spectral densities are releted by

$$S_{T_s} = S_T + (.51\overline{T})^2 S_q \pm 1.01\,\overline{T}\quad S_q S_T$$

In most cases, the terms involving fluctuations of q were small, so that S_{T_s} should be nearly equal to S_T. Fig. 7 compares typical spectra of T and T_s for a case of small moisture variation. Clearly, the agreement is poor, especially in the inertial range, where the sonic spectra remain high when they should decay rapidly with frequency. This difference is

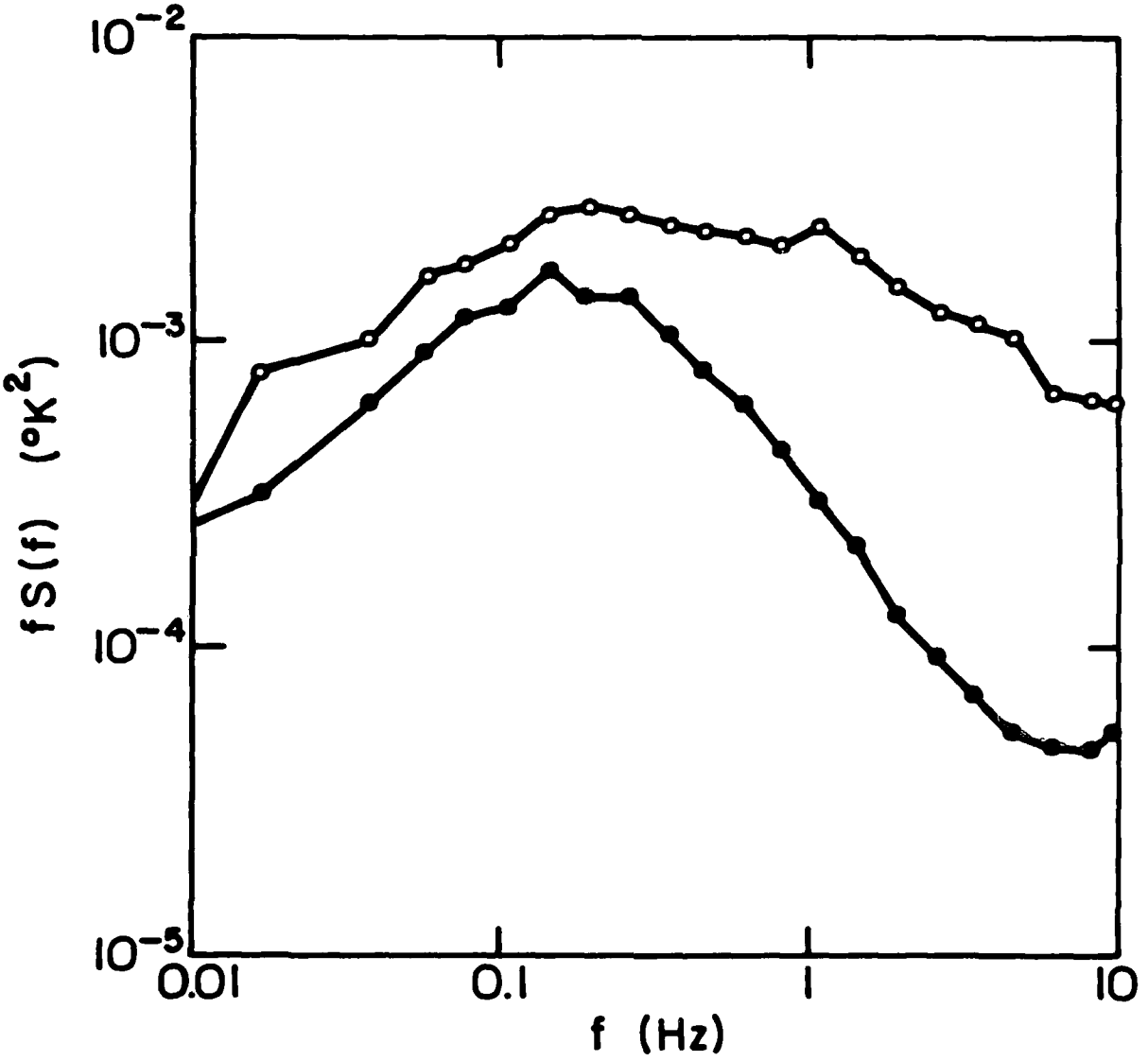

Fig. 7 Comparison of one-dimensional temperature spectra for Run 21-1 from cold wire (dots) and sonic thermometer (circles). $\overline{w'q'}$ for this run was small.

most likely caused by "noise" in the sonic data, and has the consequence that C_T^2, and therefore, C_N^2 for sound could not be determined from the sonic spectra.

The hypotheses that high-frequency variations of sonic temperature are noisy is confirmed by the chaotic behavior of high frequencies of the cospectra between sonic temperature and moisture. Therefore, we could not evaluate C_N^2 (for sound) independently from C_T^2, to test equations (6) or (9).

Another question associated with these equations is the correlation between high-frequency variations of moisture and temperature. If this correlation is + 1 or - 1, these equations become identical.

Observations indeed show numerically large correlations between temperture and moisture which, however, decrease toward high frequencies. This may be because moisture and temperature are not measured at the same location. It seems intuitively reasonable that high frequency temperature and moisture fluctuations at a fixed location should be well correlated since they are presumably produced by the same high-frequency vertical velocities.

4.6 C_q^2

Figure 8 compares bulk estimates of C_q^2 with C_q^2 determined from moisture spectra. In stable air, the bulk methods underestimate the C_q^2 by an average of 2, and in unstable air, bulk methods tend to overestimate the C_q^2 by an average factor of 1.7, at least for cases in which bulk heat flux and local heat flux at 10 m have the same sign. Also, in unstable air, the scatter is quite large. But on the average, the agreement is reasonably good.

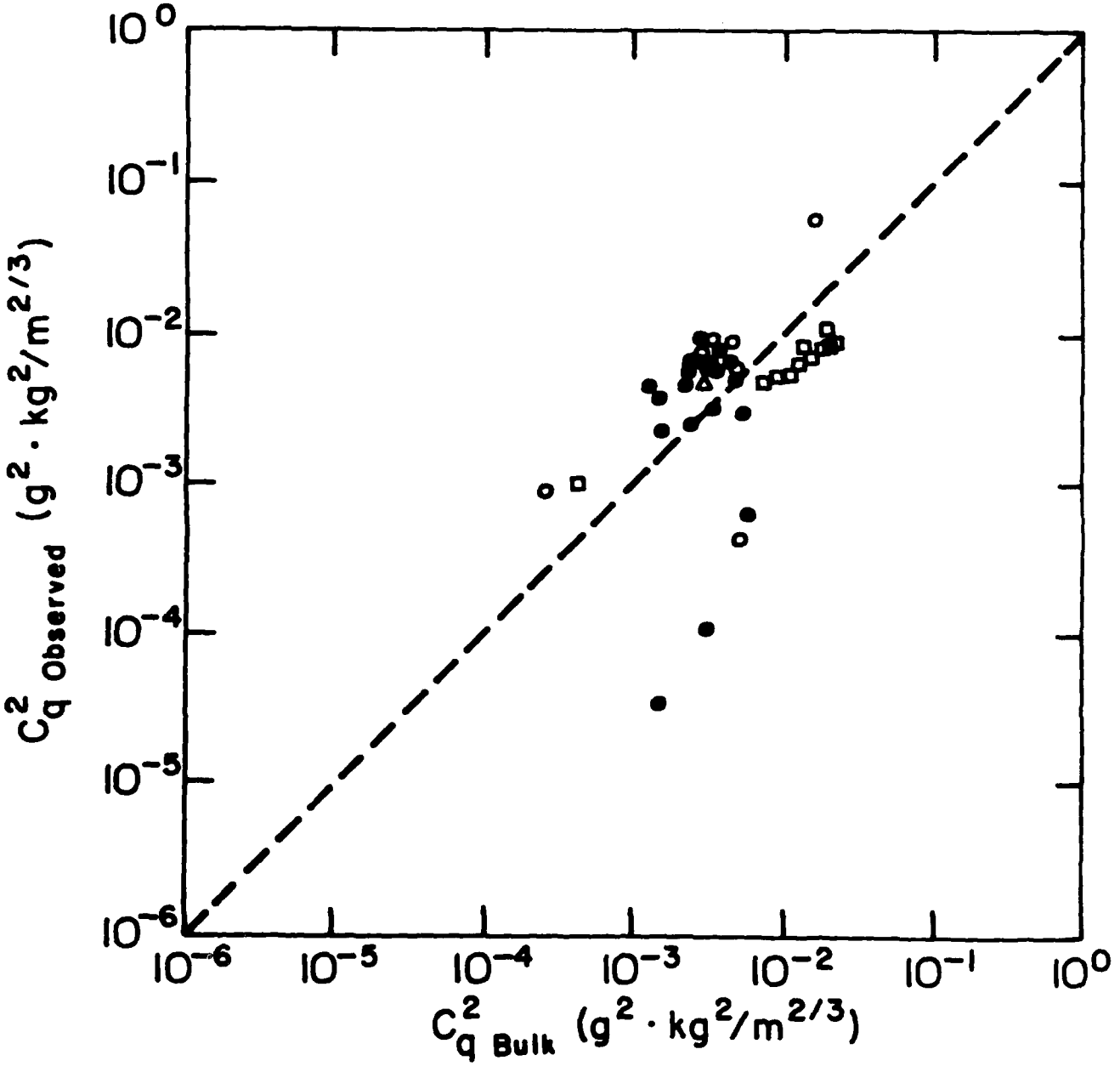

Fig. 8 Comparison of moisture structure constants from one-dimensional moisture spectra and the bulk method. Symbols as in fig. 6.

We can write C_q^2 in analogy with C_T^2:

$$C_q^2 = q_*^2 z^{-2/3} g(z/L)$$

In order to try to understand the different effect of stability on bulk C_q^2 and spectral C_q^2, we have further analyzed the behavior of $g(z/L)$.

We had previously suggested that $g(z/L)$ is the same funcation as $f(z/L)$ in equ. 6. We have now recomputed $g(z/L)$ from the spectral observations of C_q^2, and show it in Fig. 9 as function of z/L. Apparently, it differs significantly from Wyngaard et al.'s (1971) $f(z/L)$; and it differs in the opposite sense as $f(z/L)$ computed by Fairall et al. (1980). This difference may be due to the overestimate of u_*^3 by the bulk method noted earlier, resulting in an overestimate in the absolute value of L. This means that the bulk method underestimates $|z/L|$. If we increased $|z/L|$ by a factor of 3 (as suggested by fig. 3) the agreement between Wyngaard's equation and the curve inferred from the present data would be quite good. However, we must remember that the stress comparison excluded most of the unstable cases.

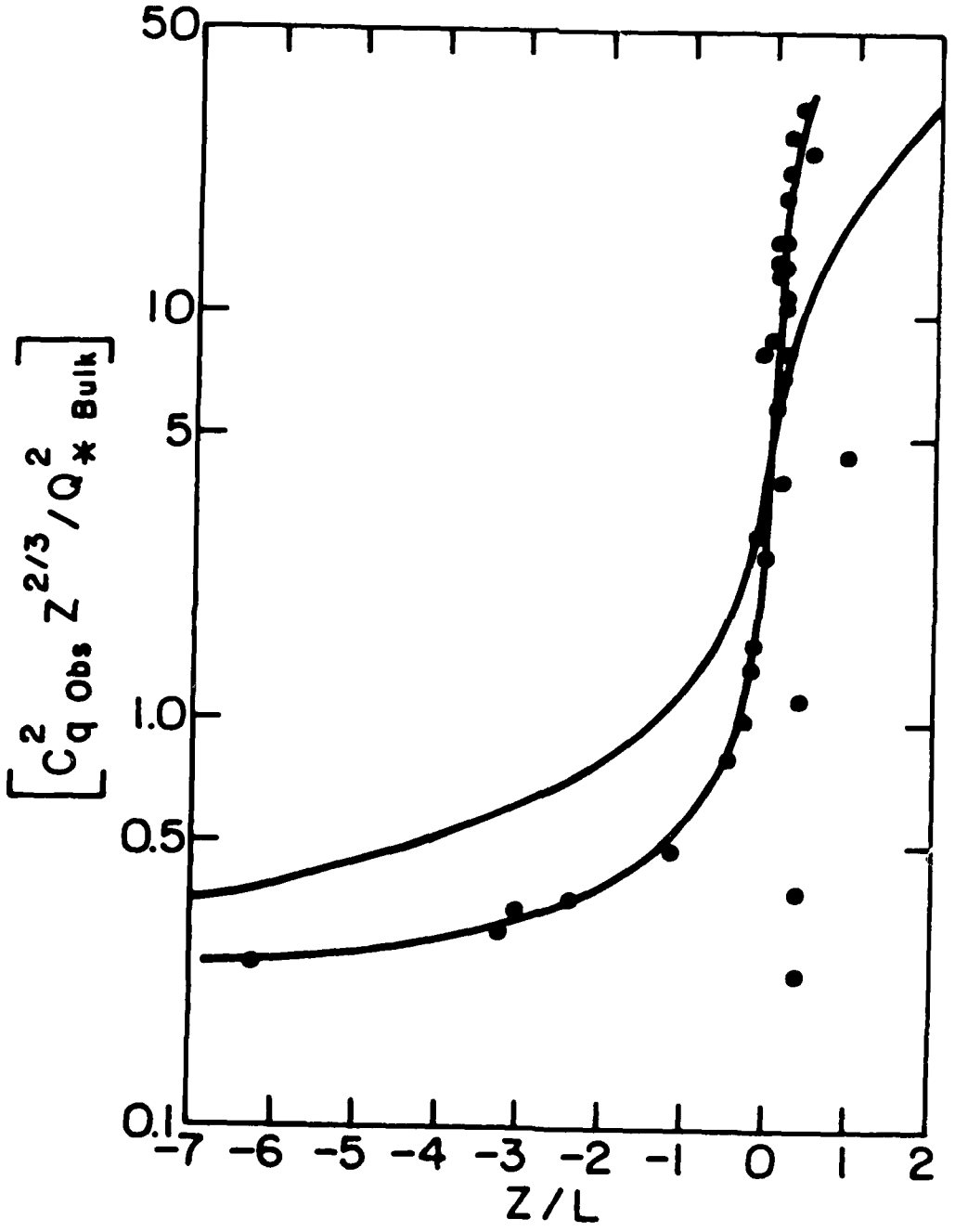

Fig. 9 $g(\frac{z}{L})$ according to Wyngaard (solid line); dots from observed C_q^2 and bulk Q_*^2; second solid line drawn to dots.

5. Summary

Observations of means and fluctuations of wind components and temperature on masts over Lake Ontario have been used to evaluate bulk methods for estimating C_T^2, and fluxes of momentum heat and moisture. The observations extended from generally stable conditions in May to unstable conditions in October.

C_T^2 was directly determined from temperature spectra in the inertial range; the fluxes were estimated by the product-momentum method. In addition, stresses could be determined from the spectra of the longitudinal wind components in the inertial range.

Stresses determined by the two methods based on wind fluctuations agreed quite well with each other, but stresses estimated from mean winds and drag coefficients were significantly larger for strong winds and large fetches. In other words, the drag coefficients assumed from previous work were much too large.

Observed and bulk heat fluxes agreed quite well. There were, however, a few cases of weak heat flux when the signs derived from the two methods were inconsistent. In these cases, the local lapse rate at 10 m was stable (hence $\overline{w'T'} < 0$); but the lake surface temperatures were larger than the temperatures at 10 m (hence upward bulk flux). Here the vertical structure was nonhomogeneous, probably due to the relatively warm Niagara plume; in these cases, the conditions for use of the bulk methods were violated.

Bulk and direct estimates of moisture flux agreed quite well, however, with considerable random scatter.

Directly measured and bulk methods for estimation of C_T^2 agreed surprisingly well, except in a few cases of small C_T^2 where the signs of the bulk heat fluxes were incorrect.

The agreement was good even for strong winds and large fetch, when the drag coefficients used seriously overestimated the stresses.

It is shown that, in strong winds, drag coefficients (for momentum) have little effect on C_T^2.

C_N^2 could not be measured directly; but the measurement of the fluxes over Lake Ontario and theoretical argument suggest that moisture only rarely affected C_N^2, so that C_N^2 was essentially proportional to C_T^2 at this site.

6. Acknowledgment

The author's would like to thank Dr. Mark Donelan of the Canadian Center of Inland Waters for permission to use his excellent observations, and for constant help in their reduction and interpretation of the results.

References

Burk, S.D., A.K. Goroch, A.I. Weinstein, and H.A. Panofsky, 1979: Modeling the refractive index structure parameter in the marine planetary boundary layer. NEPRF Technical Report TR 79-03.

Davidson, K.L., G.E. Schacher, C.W. Fairall, and A.K. Goroch, 1981: Verification of the bulk model for calculating overwater optical turbulence. Applied Optics, 20, 2919-2924.

Donelan, MA.A, K.N. Birch, and D.C. Beesley, 1974: Generalized profiles of wind speed, temperature, and humidity. Internat. Assoc. Great Lakes Res., Conf. Proc. 17, 369-388.

Fairall, C.W., G.E. Schacher, and K.L. Davidson, 1980: Measurements of the humidity structure function parameters C_q^2 and C_{Tq} over the ocean. Boundary Layer Meteor., 19, 81-92-

Garrett, J.R., 1977: Review of drag coefficients over oceans and continents. Mon. Wea. Rev., 105, 915-929.

Liu, W.T., K.B. Katsaros, and J.A. Businger, 1979: Bulk parameterization of air-sea exchanges of heat and water vapor including the molecular constraints at the inferface. J. Atmos. Sci., 36, 1722-1735.

McIlveen, J.F.R., 1981: The potential importance of correlated humidity and temperature variations for atmcspheric acoustic backscatter. J. Applied Meteor., 20, 206-209.

Mitsuta, Y., 1966: Sonic anemometer-thermometer for general use. J. Meteor. Soc. Japan, Ser. II, 44, 12-24.

Smith, J.D., 1974: Eddy flux measurements over Lake Ontario. Boundary Layer Meteor., 6, 235-255.

Smith, S.D., and E.G. Banke, 1975: Variation of the sea surface drag coefficient with wind speed. Quart. J. Roy. Meteor. Soc., 101, 665-673.

Tatarski, V.I., 1971: The effects of the turbulent atmosphere on wave propagation. Translated by Keter Press, Jerusalem, NTIS TT, 68-50464.

Wesley, M.L., 1976: The combined effect of temperature and humidity fluctuations on refractive index. J. Applied Meteor., 15, 43-49.

Wyngaard, J.C., Y. Izumi, and S.A. Collins, Jr., 1971: Behavior of the refractive index-structure parameter near the ground. J. Opt. Soc. Amer., 61, 1646-1650.

DISTRIBUTION

COMMANDING OFFICER
NAVAL RESEARCH LAB
ATTN: LIBRARY, CODE 2620
WASHINGTON, DC 20390

OFFICE OF NAVAL RESEARCH
EAST/CENTRAL REGIONAL OFFICE
BLDG. 114, SECT. D
459 SUMMER ST.
BOSTON, MA 02210

COMMANDING OFFICER
OFFICE OF NAVAL RESEARCH
1030 E. GREEN ST.
PASADENA, CA 91101

OFFICE OF NAVAL RESEARCH
SCRIPPS INSTITUTION OF
OCEANOGRAPHY
LA JOLLA, CA 92037

COMMANDING OFFICER
NORDA, CODE 101
NSTL STATION
BAY ST. LOUIS, MS 39529

COMNAVOCEANCOM
ATTN: J.W. OWNBEY
CODE N542, NSTL STATION
BAY ST. LOUIS, MS 39529

COMMANDING OFFICER
NAVOCEANO LIBRARY
NSTL STATION
BAY ST. LOUIS, MS 39522

COMMANDING OFFICER
FLENUMOCEANCEN
MONTEREY, CA 93940

CHAIRMAN
OCEANOGRAPHY DEPT.
U.S. NAVAL ACADEMY
ANNAPOLIS, MD 21402

COMMANDER (2)
NAVAIRSYSCOM
ATTN: LIBRARY (AIR-0004)
WASHINGTON, DC 20361

COMMANDER
NAVAIRSYSCOM (AIR-33)
WASHINGTON, DC 20361

COMMANDER
NAVAIRSYSCOM
MET. SYS. DIV. (AIR-553)
WASHINGTON, DC 20360

COMMANDER
NAVAIRSYSCOM (AIR-03)
NAVY DEPT.
WASHINGTON, DC 20361

COMMANDER (5)
NAVAL SEA SYSTEMS COMMAND
ATTN: LCDR S. GRIGSBY
PMS-405/PM-22
WASHINGTON, DC 20362

COMMANDER
NAVAIRDEVCEN (3011)
ATTN: N. MACMEEKIN
WARMINSTER, PA 18974

SUPERINTENDENT
LIBRARY REPORTS
U.S. NAVAL ACADEMY
ANNAPOLIS, MD 21402

COMMANDER
NAVOCEANSYSCEN
DR. J. RICHTER, CODE 532
SAN DIEGO, CA 92152

COMMANDER
NAVAL WEAPONS CENTER
DR. A. SHLANTA, CODE 3918
CHINA LAKE, CA 93555

COMMANDER
NAVAL SURFACE WEAPONS CENTER
DR. B. KATZ, WHITE OAKS LAB
SILVER SPRING, MD 20910

DIRECTOR
NAVSURFWEACEN, WHITE OAKS
NAV SCIENCE ASSIST. PROGRAM
SILVER SPRING, MD 20910

COMMANDER
PACMISTESTCEN
GEOPHYSICS OFFICER, CODE 3250
PT. MUGU, CA 93042

NAVAL POSTGRADUATE SCHOOL
METEOROLOGY DEPT., CODE 63
MONTEREY, CA 93940

NAVAL POSTGRADUATE SCHOOL
OCEANOGRAPHY DEPT., CODE 68
MONTEREY, CA 93940

LIBRARY
NAVAL POSTGRADUATE SCHOOL
MONTEREY, CA 93940

COMMANDER
AWS/DN
SCOTT AFB, IL 62225

USAFETAC/TS
SCOTT AFB, IL 62225

AFGL/LY
HANSCOM AFB, MA 01731

AFOSR/NC
BOLLING AFB
WASHINGTON, DC 20312

COMMANDING OFFICER
U.S. ARMY RESEARCH OFFICE
ATTN: GEOPHYSICS DIV.
P.O. BOX 12211
RESEARCH TRIANGLE PARK, NC 27709

COMMANDER & DIRECTOR
U.S. ARMY ATMOS. SCIENCES LAB
ATTN: DELAS-EO
WSMR, NEW MEXICO 88002

DIRECTOR (12)
DEFENSE TECHNICAL INFORMATION
CENTER, CAMERON STATION
ALEXANDRIA, VA 22314

DIRECTOR
OFFICE OF ENV. & LIFE SCIENCES
OFFICE OF THE UNDERSEC. OF
DEFENSE FOR RSCH & ENG, E&LS
RM. 3D129, THE PENTAGON
WASHINGTON, DC 20505

FEDERAL COORDINATOR FOR
METEORO. SVCS & SUPPORT RSCH
(OFCM), SUITE 300
ROCKVILLE, MD 20852

DIRECTOR
OFFICE OF PROGRAMS RX3
NOAA RESEARCH LAB
BOULDER, CO 80302

DIRECTOR
GEOPHYS. FLUID DYNAMICS LAB
NOAA, PRINCETON UNIV.
P.O. BOX 308
PRINCETON, NJ 08540

DR. E. W. FRIDAY, DEP. DIR.
NATIONAL WEATHER SERVICE
GRAMAX BLDG.
8060 13TH ST.
SILVER SPRING, MD 20910

HEAD, ATMOS. SCIENCES DIV.
NATIONAL SCIENCE FOUNDATION
1800 G STREET, NW
WASHINGTON, DC 20550

LABORATORY FOR ATMOS. SCIENCES
NASA GODDARD SPACE FLIGHT CENTER
GREENBELT, MD 20771

SCRIPPS INSTITUTION OF
OCEANOGRAPHY, LIBRARY
DOCUMENTS/REPORTS SECTION
LA JOLLA, CA 92037

CHAIRMAN, METEOROLOGY DEPT.
PENN STATE UNIVERSITY
503 DEIKE BLDG.
UNIVERSITY PARK, PA 16802

UNIVERSITY OF WASHINGTON
ATMOSPHERIC SCIENCES DEPT.
SEATTLE, WA 98195

COLORADO STATE UNIVERSITY
ATMOSPHERIC SCIENCES DEPT.
ATTN: LIBRARIAN
FT. COLLINS, CO 80521

NAUTILUS PRESS, INC.
WEATHER & CLIMATE REPORT
1056 NATIONAL PRESS BLDG.
WASHINGTON, DC 20045

PACIFIC SIERRA RSCH. CORP.
ATTN: A. SHAPIRO
1456 CLOVERFIELD BLVD.
SANTA MONICA, CA 90404

ARVIN/CALSPAN ADVANCED
TECH. CENTER
ATMOS. SCI./ENV. SCI. DEPT.
P.O. BOX 400
BUFFALO, NY 14225

AMERICAN METEORO. SOCIETY
METEORO. & GEOASTRO. ABSTRACTS
P.O. BOX 1736
WASHINGTON, DC 20013

INSTITUT FUR METEOROLOGIE
JOHANNES GUTENBERG UNIVERSITAT
ATTN: DR. R. JAENICKE
D-65 MAINZ
FEDERAL REPUBLIC OF GERMANY

MICROFISICA DELL' ATMOSFERA
CONSIGLIO NAZIONALE DEL RICERCHE
BOLOGNA, 40126, ITALY

END

DATE
FILMED

DTIC